



Kontes Robot Sepak Bola Beroda

Tugas Akhir

Oleh:

Muhammad Imron Shodiq (4222101009)

Rizqy Pratama Singarimbun (4222101004)

Program Studi Teknik Robotika

Jurusan Teknik Elektro

Politeknik Negeri Batam

2025

Pernyataan Keaslian Tugas Akhir

Saya yang bertandatangan dibawah ini menyatakan bahwa isi sebagian maupun keseluruhan Tugas Akhir saya yang berjudul : "Performance Comparison of Wheeled Soccer Robot Frames Using Finite Element Analysis (FEA)", dan "Performance Comparison of YOLOv5, YOLOv8, and YOLOv10 for Object Detection in Autonomous Soccer Robots" adalah hasil karya sendiri, diselesaikan tanpa menggunakan bahan-bahan yang tidak diizinkan, dan bukan merupakan karya pihak lain yang saya akui sebagai karya sendiri. Semua referensi yang dikutip atau dirujuk telah ditulis secara lengkap pada daftar pustaka. Apabila ternyata pernyataan saya ini tidak benar, saya bersedia menerima sanksi sesuai peraturan yang berlaku.

Batam, 09 Januari 2025



Rizqy Pratama Singarimbun
NIM: 4222101004



Muhammad Imron Shodiq
NIM: 4222101009

Lembar Pengesahan

Tugas Akhir disusun untuk memenuhi salah satu syarat memperoleh gelar
Sarjana Terapan Teknik (S.Tr.T)
di
Politeknik Negeri Batam

Oleh:
Muhammad Imron Shodiq (4222101009)

Dengan judul:
Performance Comparison of Wheeled Soccer Robot Frames Using Finite Element Analysis (FEA)

Tanggal Sidang: 15 01, 2025

Disetujui oleh :

Dosen Penguji I



1. Hendawan Soebhakti, S.T., M.T.
NIK : 104031

Dosen Pembimbing I



1. Anugerah Wibisana S.Tr.T, M.Tr.T
NIK: 122287

Dosen Penguji II



2. Ryan Satria Wijaya, S.Tr.T, M.Tr.T.
NIK : 121249

Lembar Pengesahan

Tugas Akhir disusun untuk memenuhi salah satu syarat memperoleh gelar
Sarjana Terapan Teknik (S.Tr.T)
di
Politeknik Negeri Batam

Oleh:
Rizqy Pratama Singarimbun (4222101004)

Dengan judul:
Performance Comparison of YOLOv5, YOLOv8, and YOLOv10 for Object Detection in Autonomous
Soccer Robots

Tanggal Sidang: 15 01, 2025

Disetujui oleh :

Dosen Penguji I



1. Hendawan Soebhakti, S.T., M.T.
NIK : 104031

Dosen Pembimbing I

A handwritten signature in black ink, located below the name of the first supervisor, Anugerah Wibisana.

1. Anugerah Wibisana S.Tr.T, M.Tr.T
NIK: 122287

Dosen Penguji II

A handwritten signature in black ink, located below the name of the second examiner, Ryan Satria Wijaya.

2. Ryan Satria Wijaya, S.Tr.T, M.Tr.T.
NIK : 121249

Performance Comparison of Wheeled Soccer Robot Frames Using Finite Element Analysis (FEA)

Muhammad Imron Shodiq^{1*} and Anugerah Wibisana¹

¹ Department of Electrical Engineering, Batam State Polytechnic, Batam, Indonesia

* Email: m.imron@students.polibatam.ac.id

Abstract—Frame analysis is critical in the Indonesian Wheeled Football Robot Contest (KRSBI-B) because, through this analysis, the weaknesses of the design can be identified and optimized before being applied to the real physical robot. In this study, three types of robot frame designs are evaluated: standard frames, modified standard frames, and frames designed by the Tech United team. Each design is assessed using the Finite Element Analysis (FEA) technique on SolidWorks software to evaluate stress, displacement, and Factor of Safety (FOS). Vertical load pressure of 25 kg, equivalent to five times the robot's upper base load, and horizontal load pressure of 80 kg, equivalent to twice the robot's maximum weight as stated in the national competition rulebook, are applied. The analysis results indicate that the Tech United frame exhibits superior performance, with a stress value of 5.8 MPa under vertical load pressure and 180.0 MPa under horizontal load pressure, a smaller displacement of 0.018 mm vertically and 1.806 mm horizontally, and a FOS value of 9.5 for vertical load and 0.3 for horizontal load. Furthermore, the highest stiffness, exceptional stability, and a controlled damage zone, where deformation is concentrated in specific areas designed to absorb impact, are demonstrated by the Tech United frame. These features enhance the frame's durability and reliability, establishing the optimal choice for improving the robot's performance and ensuring robustness under competitive conditions.

Keywords: *Finite Element Analysis* , *Factor Of Safety* , wheeled soccer robot , aluminum 6061.

I. INTRODUCTION

INDONESIA Robot Contest is an annual robotics competition in Indonesia with several categories, one of which is the Indonesian Wheeled Football Robot Contest based on the international competition RoboCup Middle Size League as the initiator. This competition allows students to develop student abilities in various fields, such as mechanics, manufacturing, electronics, and programming. The competition demands that wheeled robots as football players to coordinate, communicate, and play football autonomously, like human football in general [1], [2].

In the Indonesia Robot Contest, the weight of the components and robot base often creates vertical load pressure that affects the condition of the robot frame, both in static and dynamic conditions, and the enemy's robot may collide with

the robot that will creates horizontal load pressure which poses a risk of stress and material displacement. because of this, the developed robot must have high resistance, especially in the foundation or frame section of the robot, which is an important factor in supporting the frame to keep the frame prevent damage and changes in shape due to impact within a vertically and horizontally load pressure [3]. Therefore, researchers aim to design a robot frame that is as strong as possible and can withstand the vertical load pressure of components and the risk of impact caused by the horizontal load pressure as effectively as possible.

The robot frame design was created using Computer-Aided Design (CAD) software Solidworks 2020, which supports precision design and allows structural strength analysis with the Finite Element Analysis (FEA) feature [4]. FEA is a numerical analysis method that divides the design into small elements, called nodes, through the meshing process. In Solidworks, the feature used is static analysis [5], [6], [7].

This analysis aims to enable virtual testing of robot frame design variations to identify and correct design weaknesses before implementation in real physical robots. With this optimization, the frame is expected to avoid excessive stress that can cause deformation and structural failure during the game and ensure that the frame has an adequate level of safety with the Factor of Safety (FOS) generated from the simulation [7], [8], [9], [10].

The material used in the simulation is aluminum 6061 and three frame designs to be compared: the first frame is the standard frame used in current robots, the second frame is a modification of the standard design; and the third frame is the frame design of the Tech United team from Eindhoven [11]. The results of this analysis are expected to contribute to the optimization of the robot design, both in terms of durability and material efficiency.

II. METHOD

This research begins with designing a wheeled soccer robot frame to implement an optimal and efficient frame design during the competition. Figure 1 shows the flow diagram of this research process, which has several stages which will be explained as follows:

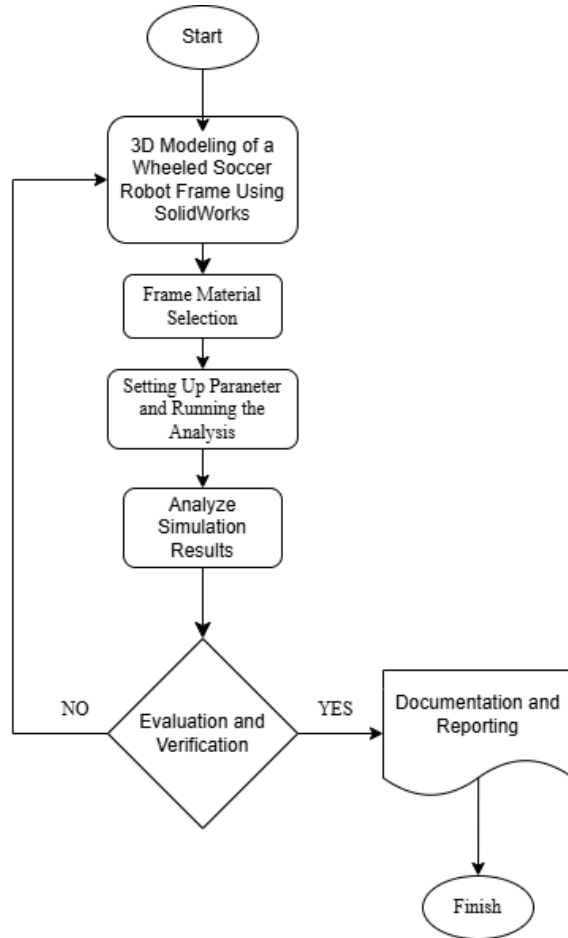


Fig. 1. Flow diagram

A. 3D Modeling of Wheeled Football Robot Frame

The 3D modeling of the wheeled soccer robot frame begins with a design concept that meets the needs of the Indonesia Robot Contest, such as durability. The frame is designed to withstand movements that put excessive pressure on the structure. Therefore, the frame structure must have sufficient strength to support all robot components. Various frame designs are evaluated in this design process to find the best design. The 3D frame model design is made with the help of CAD software, namely Solidworks 2020. The process of making this model involves determining the size and layout of each part of the structure, including joints. Each component is planned with strength, stability, and load distribution in mind to withstand intense use during the match.

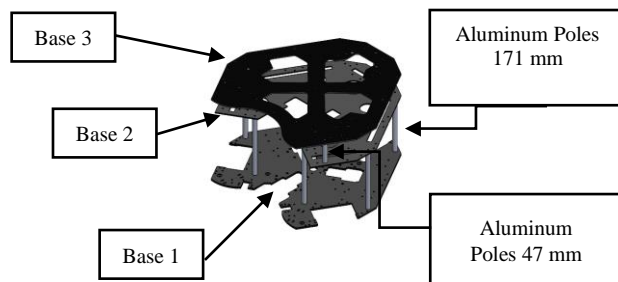


Fig. 2. Isometric view of Standard frame

The standard frame design shown in Figure 2 consists of three layers of aluminum base plates supported by nine aluminum poles. Six aluminum poles connect the first and second layers with a length of 171 mm and for the second and third layers are connected by 47 mm aluminum poles.

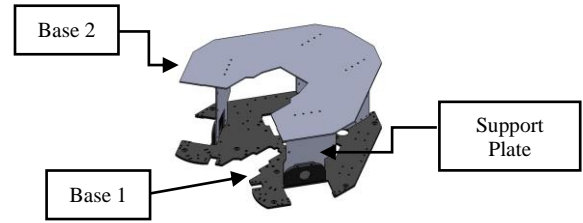


Fig. 3. Isometric view of Modified frame

Figure 3 show the modified frame design from a standard frame. The design uses supports from 4 aluminum plates connected to the second layer base plate using L-shape angles aluminum.

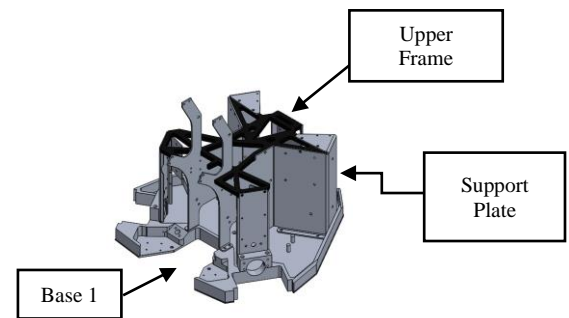


Fig. 4. Isometric view of Tech United frame

Figure 4 shows the Tech United's frame which uses five aluminum plates as the top frame support.

B. Frame Material Selection

Choosing the right material is essential to balancing strength and weight in a robot frame. This research uses aluminum 6061, known for the high strength, durability, and lightweight properties. The excellent strength-to-weight ratio and machinability make the material ideal for structural applications like robot frames. Compared to aluminum 5052, aluminum 6061 has higher tensile and yield strength, allowed the material to handle greater loads and stress without deforming. While 5052 is more corrosion-resistant [12], 6061's superior strength makes material better suited for high-performance robot designs.

SolidWorks data for 6061 aluminum shows key material properties. With a modulus of elasticity of 69,000 N/mm², the material is stiff and does not deform easily under pressure. A Poisson's ratio of 0.33 indicates moderate lateral contraction under axial compression. A shear modulus of 26,000 N/mm² indicates the material's strength under shear loads. The density of 6061 aluminum is 2,700 kg/m³, making the material is a

lightweight yet strong material. 6061 aluminum has a high tensile strength of 124,084 N/mm² and a yield strength of 55.1485 N/mm², making this capable of withstanding heavy loads without breaking. A coefficient of thermal expansion of 2.4e-05/K indicates that will expanded moderately with temperature changes. and 170 W/(m K) thermal conductivity means material can dissipate heat efficiently. With a specific heat of 1300 J/(kg·K), the material requires much energy for temperature changes, which is important for thermal stability. Additional information shows that aluminum 6061 is very suitable for various mechanical and structural uses; the material properties can be seen in Table 1[13] .

TABLE I
ALUMINUM 6061 MATERIAL PROPERTIES

Properties	Value	Units
Elastic Modulus	69000	N/mm ²
Poisson's Ratio	0.33	N/A
Shear Modulus	26000	N/mm ²
Mass Density	2700	Kg/m ³
Tensile Strength	124,084	N/mm ²
Yield Strength	55.1485	N/mm ²
Thermal Expansion Coefficient	2.4e-05	/K

C. Setting Up Parameter and Running the Analysis .

To assess the performance of each frame design, Simulations for each frame design are conducted using SolidWorks Finite Element Analysis (FEA), focusing on stress, displacement, and factor of safety (FOS). FEA, is a numerical method, solves engineering problems like stress analysis, heat transfer, and fluid flow by dividing structures into smaller elements for precise evaluation [14].

In each simulation, the following parameters are applied, the first parameter involves inputting the material properties into the simulation, which is set as alloy 6061. The second parameter involves applying external loads, which in this simulation are divided into two types, vertical load pressure and horizontal load pressure. The vertical load pressure input is set at 5 kg, derived from the original weight of the upper base., which will be maximized by multiplied by five so that the weight inputted in the simulation is 25 kg. The second simulation results on each frame are carried out of the maximum weight of wheeled robot soccer on the national competition rules which are 40kg [2]. that will multiplied by two so the weight that the inputted in the simulation is 80kg with the horizontal direction. This approach is used to evaluate the optimal strength of the frame when facing a vertical load pressure that is five times greater than normal conditions and the horizontal load pressure two times greater on the maximum weight of the robot. The simulation results are visualized through SolidWorks through 3D models, graphs, diagrams, and data tables. The appearance of the upper Base can be seen on the right of Figure 5, and the mass properties can be seen on the left of Figure 5.

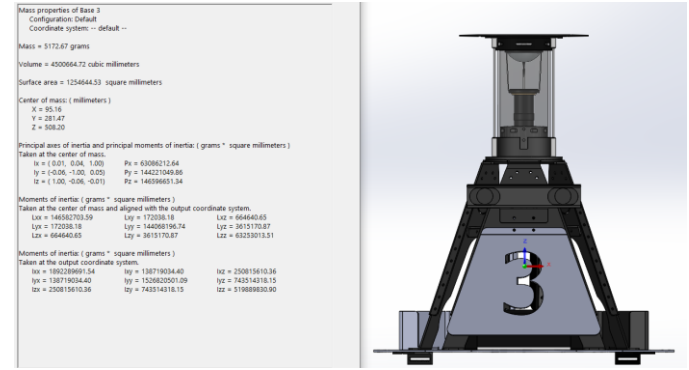


Fig. 5. Left view of mass properties and the right view of the robot's top Base .

The first simulation performed is stress analysis, which identifies the stress distribution on the frame under operational loads. This helps pinpoint high-stress areas that could lead to material failure. the stress occurring in an object can be formulated as follows:

$$\sigma = \frac{F}{A} \quad (1)$$

Where the symbol is :

σ = Stress or force per unit area (N/m²)

F = Force (N)

A = Cross-sectional area (m²)

The second simulation is displacement analysis, which evaluates how the frame deforms under load. Excessive displacement can compromise the robot's balance and stability during operation. This analysis ensures the frame maintains rigidity to maintain stability, the displacement occurring in an object can be formulated as follows:

$$E = \frac{\sigma}{\epsilon} \quad (2)$$

Where the symbol is:

E = Modulus of elasticity

σ = Stress (N/m²)

ϵ = Strain

The third simulation is the factor of safety (FOS) analysis, used to assess the safety margin of the frame under load. FOS represents the ratio between the applied stress and the material's strength before permanent deformation. This analysis highlights areas with low safety margins, guiding designers to modify or strengthen components to ensure reliability[15][16]. the FOS occurring in an object can be formulated as follows:

$$\eta = \frac{s_y}{\sigma_e} \quad (3)$$

Where the symbol is :

η = Factor of Safety

s_y = Yield strength of the material (N/m²)

σ_e = Maximum von Mises stress

III. RESULTS AND DISCUSSION

This chapter presents the simulation results and analysis of three different frame designs for a wheeled soccer robot. The evaluations include stress, displacement, and Factor of Safety (FOS) analyses under vertical and horizontal load pressures with setted parameter.

A. Stress analysis

The first test simulated is stress analysis, which is a method to determine the frame response to static loading by measuring the stress that occurs in the structure. The results of the analysis per frame from the simulation are as follows:

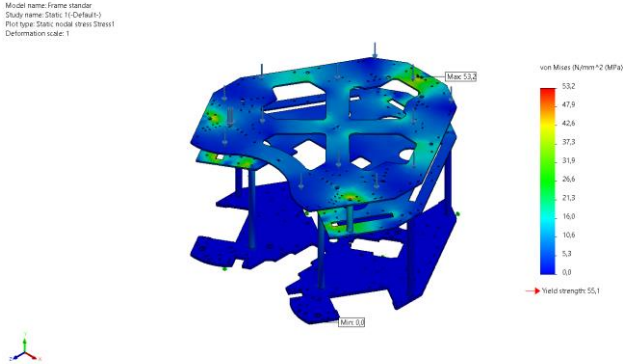


Fig .6. Vertical load stress analysis results of standard frame.

In Figure 6, this frame shows the highest stress level, 53.2 MPa caused by the vertical load pressure. This shows that the standard frame is limited in distributing the load evenly, resulting in higher stress concentrations. The significant stress in this design indicates the possibility of distortion or danger when used in heavier load situations.

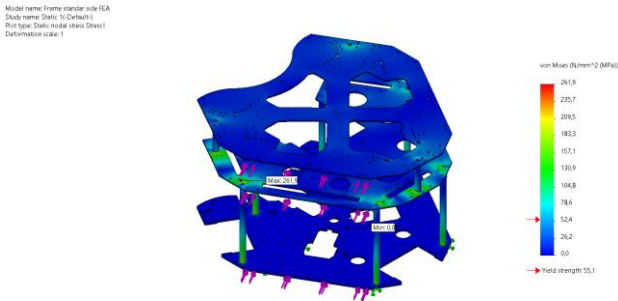


Fig .7. Horizontal load stress analysis results of standard frame.

And in figure 7, the frame shows the stress level, 261.9 MPa caused by the horizontal load pressure, The results demonstrate that the standard frame faces challenges in handling horizontal loads effectively, as the frame exhibits high stress concentrations. This significant stress suggests a heightened risk of deformation or failure when exposed to heavier horizontal loads or extreme operating conditions.

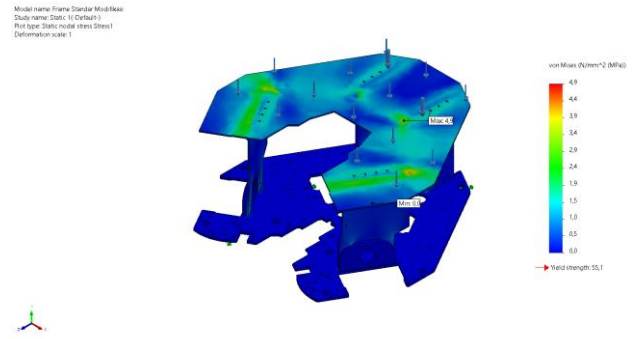


Fig.8. Vertical load stress analysis results of modified standard frame

Figure 8 shows the results of the modified standard frame. Tests show a stress of 4.9 MPa from the vertical load pressure, This frame reduces the stress level, resulting in better weight distribution, increased resistance to deformation, and frame stability in challenging operational environments.

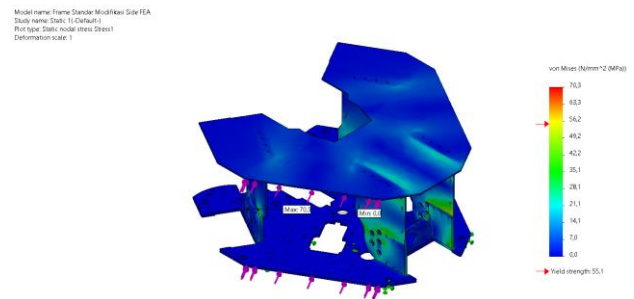


Fig.9. Horizontal load stress analysis results of modified standard frame

And In figure 9 shows a stress of 70.3 MPa from the horizontal load pressure, this indicating improved weight distribution. This design enhances resistance to deformation and ensures greater frame stability, making the frame more reliable in demanding operational environments.

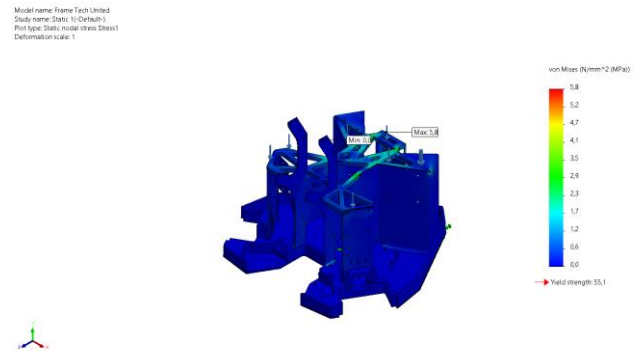


Fig. 10. Vertical load Results of stress analysis Tech United frames

In Figure 10, the Tech United frame shows a stress of 5.8 MPa caused by the vertical load pressure, this shows satisfactory load-bearing capacity performance.

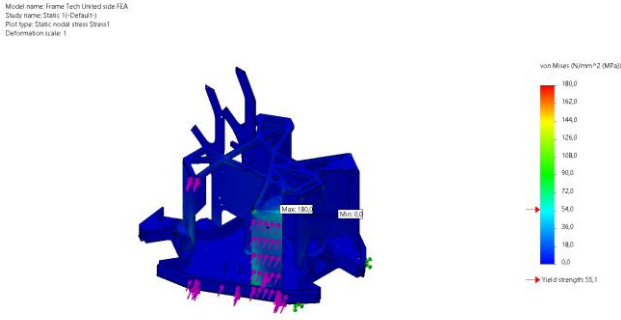


Fig. 11. Horizontal Load Results of stress analysis Tech United frames

And in Figure 11 shows a stress of 180.0 MPa caused by the horizontal load pressure. Although not as effective as the modified standard frame in distributing the load, the stress result caused by the horizontal load pressure in the frame tech united shows that the Tech United design offers increased durability and can maintain the stability of a solid structure and a focused distributed load.

TABLE II
VERTICAL STRESS ANALYSIS RESULT DATA

Frame	Value	Units
Standard Frame	53.2	N/mm ² (MPa)
Modified Standard Frame	4.9	N/mm ² (MPa)
Frame Tech United	5.8	N/mm ² (MPa)

As shown in Table II, the summarized data from the vertical stress analysis indicates that differences in frame design significantly impact the load-bearing capacity. The modified frame and the Tech United frame demonstrate better stress distribution compared to the standard frame.

TABLE III
HORIZONTAL STRESS ANALYSIS RESULT DATA

Frame	Value	Units
Standard Frame	261.9	N/mm ² (MPa)
Modified Standard Frame	70.3	N/mm ² (MPa)
Frame Tech United	180.0	N/mm ² (MPa)

Table III summarizes the data from the horizontal stress analysis, revealing that the modified standard frame exhibits the lowest stress among the designs due to focus on improved load distribution. Meanwhile, the Tech United frame demonstrates a well-distributed load pressure, effectively controlling potential damage and maintaining structural integrity.

B. Displacement analysis

In this analysis, displacement measurements are conducted for each frame design to evaluate the rigidity and stability of the robot's frame under load. The displacement value indicates the extent to which the structure shifts or deforms when subjected to external forces. Both vertical and horizontal displacement

values are analyzed to assess the frame's performance under different loading conditions. These results are critical are helped identify designs that can effectively maintain the shape and integrity under vertical pressure from components and horizontal impacts from collisions, ensuring optimal performance and durability.

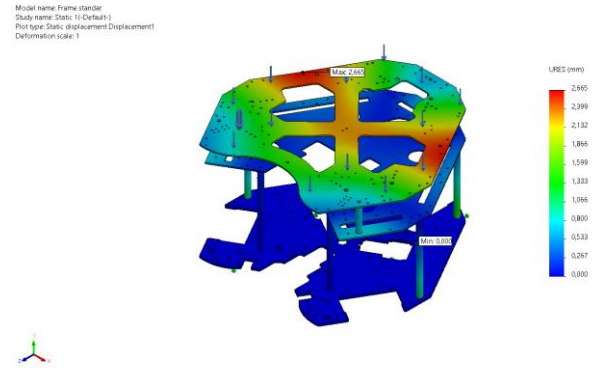


Fig. 12. Vertical load displacement analysis results standard frame

In Figure 12, the current standard frame is loaded with vertical loads, and there is a reasonably visible change in position, with a displacement value of 2,655 mm on the standard frame. This displacement value shows that the standard frame has a minor stiffness, causing the frame to deform significantly when subjected to pressure. This shows the importance of refining the design to maintain stability.

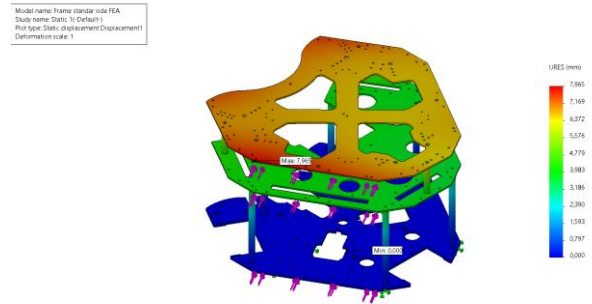


Fig. 13. Horizontal Load displacement analysis results standard frame

And in Figure 13 shows the standard frame under horizontal loading, showing a noticeable positional shift with a displacement value of 7.965 mm. This significant deformation highlights the frame's lack of stiffness, making the frame was prone to instability under pressure. These findings emphasize the need for design improvements to enhance rigidity and ensure structural stability.

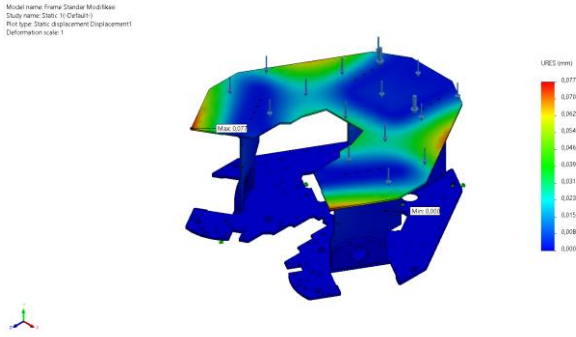


Fig. 14. Vertical load displacement analysis results of modified standard frame

In Figure 14, the modified standard frame has a displacement of 0.077 mm. This shows a significant increase in stiffness compared to the standard frame. The decreased displacement values indicate that the modified design can reduce displacement and increase resistance to deformation while maintaining structural stability under load.

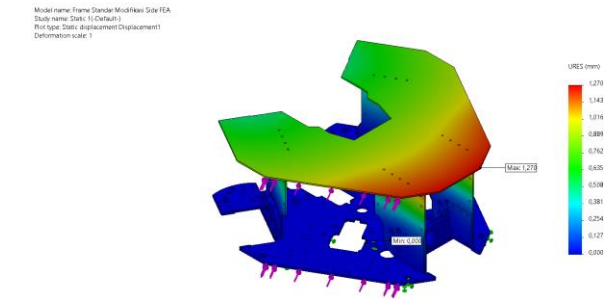


Fig. 15. Horizontal load displacement analysis results of modified standard frame

And in Figure 15, shows the modified standard frame exhibits a displacement of 1.270 mm, demonstrating a notable improvement in stiffness over the standard frame. The reduced displacement values suggest that the modified design effectively minimizes deformation, enhancing the frame's ability to resist displacement and maintain frame structural integrity under load. This indicates a stronger but with a note that the displacement point is so much distributed to the whole frame, that can causing the permanent damage of the frame.

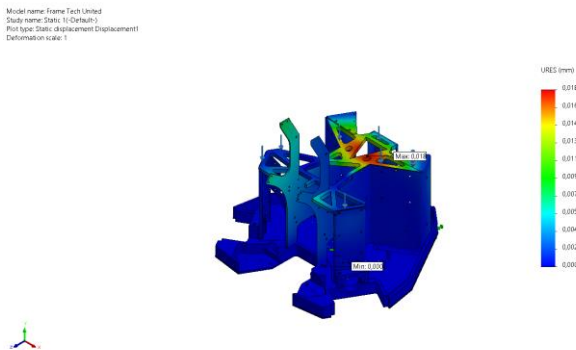


Fig. 16. Vertical load displacement analysis results of Frame Tech United

In Figure 16, the Tech United frame has the most minor displacement among the three designs; the result of the frame analysis is only 0.018 mm that caused by the vertical load. This shows that the Tech United frame is the stiffest, with an extraordinary capacity to maintain the frame shape and stability under pressure. This small displacement makes the frame be an excellent choice for designs that need to resist deformation.

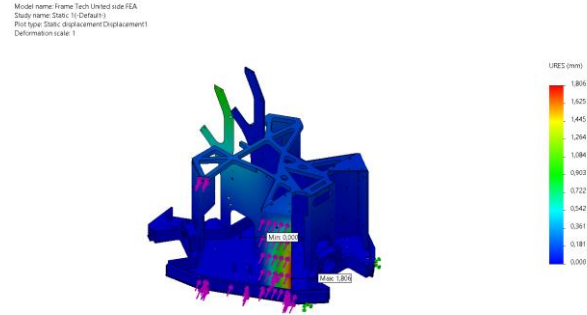


Fig. 17. Horizontal load displacement analysis results of Frame Tech United

And In Figure 17, the Tech United frame shows a displacement of 1.806 mm caused by horizontal load, placing the frame in the middle range compared to the other designs. However, despite this, the frame is designed to localize damage on the bended side plate, by that ensuring the primary structure remains unaffected. This focused distribution of displacement helps protect the core integrity of the frame while still allowing to absorb impacts effectively, makes the frame a reliable choice for maintaining stability under stress.

TABLE IV
VERTICAL LOAD DISPLACEMENT ANALYSIS RESULT DATA

Frame	Value	Units
Standard Frame	2.655	mm
Modified Standard Frame	0.077	mm
Frame Tech United	0.018	mm

In Table IV, The displacement results show that the Tech United frame outperforms the other designs in terms of stiffness under vertical load, demonstrating better stability. The displacement results show that the Tech United frame outperforms the other designs in terms of stiffness under vertical load, demonstrating better stability.

TABLE V
HORIZONTAL LOAD DISPLACEMENT ANALYSIS RESULT DATA

Frame	Value	Units
Standard Frame	7.965	mm
Modified Standard Frame	1.270	mm
Frame Tech United	1.806	mm

Additionally, for horizontal load, shows on Table V, the Tech United frame proves to be the safest although the value is greater than modified standard frame, because the frame effectively localizes damage without affecting the main structure.

C. Factor of safety (FOS) analysis

The Factor of Safety (FOS) is an important parameter in assessing a design's resistance to structural failure under a particular load. The value FOS indicates the frame's strength level in withstanding the load compared to the maximum capacity of material before experiencing deformation or damage. The higher the value FOS, the greater the margin of safety of the frame, so the frame will be more reliable and have better resistance to the risk of failure under various operational conditions.

For the standard frame, the analysis results from the vertical load pressure show that the minimum value FOS is 1.0. This value is slightly above the minimum safe limit, indicating that the standard frame is on the verge of structural failure.

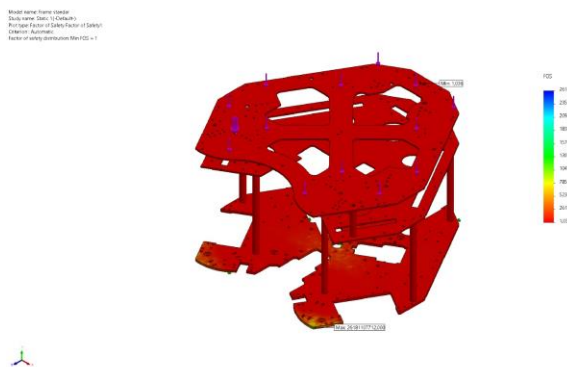


Figure .18. Vertical Load Results of standard frame analysis (FOS)

With a low FOS value, Figure 18 shows that standard frames require additional attention in the form of structural reinforcement or stronger alternative materials to increase frame durability. If improvements are not made, the risk of failure of these frames will remain high, especially in applications that require high performance and long-term durability. And using the manually calculation according to equation (3) can be obtained :

$$\text{Factor of safety} = \frac{55.15}{53.2} = 1.03$$

From that can be concluded that this simulation result is correct.

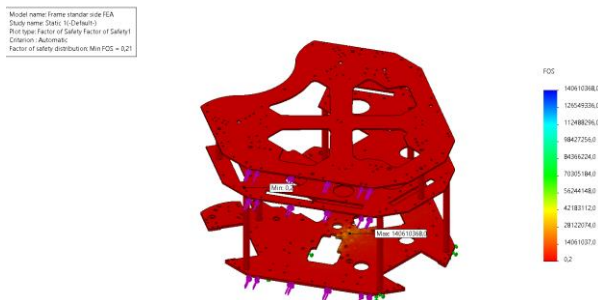


Figure .19. Horizontal Load Results of standard frame analysis (FOS)

Figure 19 Showing the Horizontal load pressure result is 0.2, This low FOS indicates that the standard frame has a fragile margin of safety, makes the frame susceptible from damages. And within the manually calculation according to equation (3) can be obtained :

$$\text{Factor of safety} = \frac{55.15}{261.9} = 0.21$$

So if compared to the manually calculation can be confirmed that this simulation result is correct.

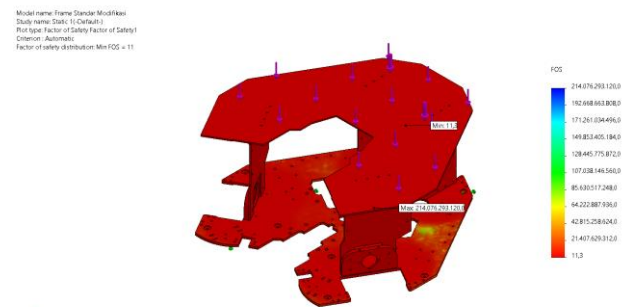


Fig. 20. Results of analysis (FOS) of modified standard frame

Figure 20 shows the modified standard frame shows that the minimum value FOS from the vertical load increased significantly to 11.3, This high value FOS indicates that the modified frame has a much larger safety margin, providing excellent resistance to structural failure even under loads higher than normal operational loads. This makes the modified standard frame more reliable and durable than the standard frame. And using the manually calculation according to equation (3) can be obtained :

$$\text{Factor of safety} = \frac{55.15}{4.9} = 11.25$$

Comparing the simulation results with manual calculations confirms the accuracy.

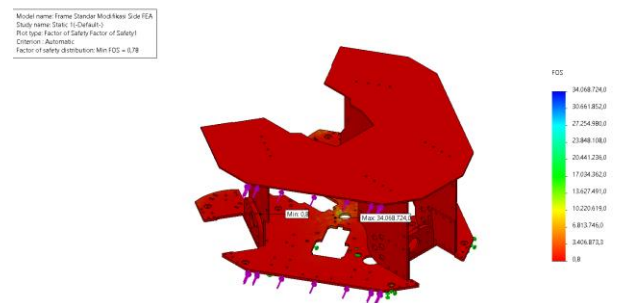


Fig. 21. Results of analysis (FOS) of modified standard frame

And in Figure 21 shows the modified standard frame, where the minimum FOS for the horizontal load has significantly increased to 0.8. This improved FOS reflects a much greater safety margin, demonstrating the frame's exceptional ability to withstand structural failure even under elevated loads beyond normal operational conditions. As a result, the modified standard frame offers more durability compared to the standard

frame. And from the manually calculation according to equation (3) can be obtained :

$$\text{Factor of safety} = \frac{55.15}{70.3} = 0.78$$

Based on the calculation the simulation output aligns well with the manual computations, validating the correctness.

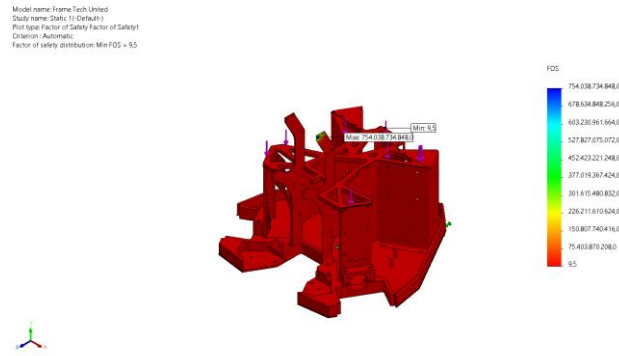


Fig. 22. Vertical Load Results of analysis (FOS) of Tech United frame

Figure 22 shows the Tech United frame design has a minimum value FOS of 9.5, showing the frame's ability to withstand loads with a fairly high safety margin. Although slightly below the modified standard frame, the Tech United frame still has excellent resistance to structural failure and is able to maintain structural performance under the vertical load conditions. And from the manually calculation according to equation (3) can be obtained :

$$\text{Factor of safety} = \frac{55.15}{5.8} = 9.50$$

By matching the simulation data with manual calculations, this verified the accuracy of the results.

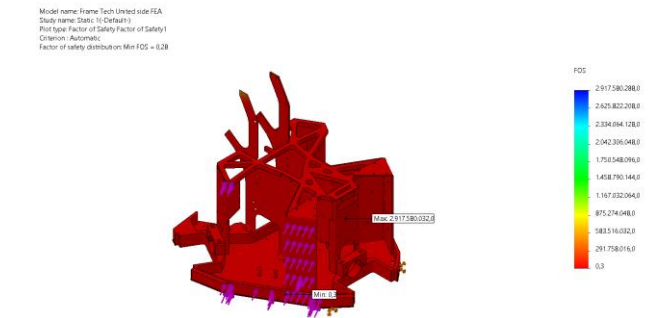


Fig. 23. Horizontal Load Results of analysis (FOS) of Tech United frame

And Figure 23 shows the Tech United frame design with a minimum FOS value of 0.3, indicating frame ability to endure horizontal loads with a modest safety margin. While slightly lower than the modified standard frame, the Tech United frame demonstrates strong resistance to structural failure and maintains reliable performance under horizontal load conditions. The lower FOS is attributed to the load concentration on the pre-bent sections, which effectively absorbs and redistributes the impact, enhancing the frame's overall load-handling efficiency. And within the manually calculation according to equation (3) can be obtained :

$$\text{Factor of safety} = \frac{55.15}{180.0} = 0.30$$

The results from the simulation correspond to the manual calculations, proving the reliability.

TABLE VI
VERTICAL LOAD FOS ANALYSIS RESULT DATA

Frame	FOS
Standard Frame	1.0
Modified Standard Frame	11.3
Frame Tech United	9.5

The FOS analysis shows that the modified standard frame and Tech United have a higher safety margin than the standard frame, making them a safer choice for applications requiring resistance to heavy loads,

TABLE VII
HORIZONTAL LOAD FOS ANALYSIS RESULT DATA

Frame	FOS
Standard Frame	0.2
Modified Standard Frame	0.8
Frame Tech United	0.3

The FOS analysis shows that the modified standard frame and Tech United have a higher safety margin than the standard frame, making them a safer choice for applications requiring resistance to heavy loads,

TABLE VIII
VERTICAL LOAD ANALYSIS RESULT DATA

Frame Design	Stress	Displacement	FOS
Standard Frame	53.2 MPa	2,655 mm	1.0
Modified Standard Frame	4.9 MPa	0.077 mm	11.3
Frame Tech United	5.8 MPa	0.018 mm	9.5

Table VIII showing all the analysis results under vertical load pressure, with the Tech United frame outperforming the others. The frame achieves the lowest stress 5.8 MPa, minimal displacement 0.018 mm, and a high FOS 9.5, demonstrating a focused load distribution, best stiffness, and a robust safety margin. This makes the Tech United frame the most reliable choice for durability and performance.

TABLE IX
HORIZONTAL ANALYSIS RESULT DATA

Frame Design	Stress	Displacement	FOS
Standard Frame	261.9	7.965 mm	0.2
Modified Standard Frame	70.3	1.270 mm	0.8
Frame Tech United	180.0	1.806 mm	0.3

Table IX showing all the analysis results under horizontal load pressure, where the Tech United frame stands out. The frame achieves moderate stress 180.0 MPa, controlled displacement 1.806 mm, and an FOS of 0.3, with deformation

concentrated in specific areas. These characteristics make the Tech United frame the most reliable option for maintaining stability and durability under horizontal loads.

IV. CONCLUSION

This research evaluates the performance of three wheeled soccer robot frame designs: the standard frame, the modified standard frame, and the Tech United frame, using stress, displacement, and Factor of Safety (FOS) analyses under vertical 25 kg and horizontal 80 kg load pressures

The results of the analysis show that the Tech United frame produced superior performance in terms of stress. Under the vertical load analysis, the frame showed a stress value of 5.8 MPa, while for the horizontal load analysis, frame showed 180.0 MPa. These results highlight the frame's ability to handle significant loads, with reduced stress concentrations compared to other designs

The displacement analysis reveals that the Tech United frame exhibits exceptional rigidity, with a minimal displacement of 0.018 mm under vertical load and 1.806 mm under horizontal load. These values indicate that the frame is highly resistant to deformation, ensuring better structural stability under both vertical and horizontal load conditions

Regarding the Factor of Safety (FOS), the Tech United frame demonstrates a value of 9.5 under vertical load, indicating a significant safety margin. However, under horizontal load conditions, the FOS is 0.3, which is lower but still within acceptable limits, showcasing the frame's capacity to withstand forces while prioritizing controlled deformation in certain areas

Additionally, the Tech United frame demonstrates the highest stiffness, exceptional stability, and a controlled damage zone where deformation is concentrated in specific areas designed to absorb the impact. This feature enhances the frame's durability and reliability, making this frame be the best choice for optimizing the robot's performance and ensuring its robustness under competitive conditions.

REFERENCE

- [1] T. Balch, T. Schmitt, F. Schreiber, and B. Cunha, "Middle Size Robot League Rules and Regulations for 2009," 2009.
- [2] B. Kusumoputro *et al.*, "Pedoman Kontes Robot Indonesia (Kri) Pendidikan Tinggi Tahun 2024," *Kementerian. Pendidikan, Kebudayaan, Riset, dan Teknol.*, pp. 1–164, 2024.
- [3] I. G. Wiratmaja, N. A. Wigraya, and K. Purnayasa, "Analisis Tegangan Statik Dan Deformasi Frame Electric Ganesha Scooter Portable (E-Gaspol) Menggunakan Software Solidworks," *Otopro*, vol. 19, no. 1, pp. 8–17, 2023, doi: 10.26740/otopro.v19n1.p8-17.
- [4] A. Welch-Phillips, D. Gibbons, D. P. Ahern, and J. S. Butler, "What Is Finite Element Analysis?," *Clin. Spine Surg.*, vol. 33, no. 8, pp. 323–324, 2020, doi: 10.1097/BSD.0000000000001050.
- [5] M. F. Arliansyah *et al.*, "Analisa Finite Element Method (FEM) Uji Beban Pada Meja Polyethylene," *J. Jalsena*, vol. 4, no. 2, pp. 122–125, 2023.
- [6] I. Dumyati and S. Nurhaji, "Modeling dan Simulasi Finite Element Analysis pada Segitiga T Sepeda Motor Menggunakan Software Ansys 2023," *Quantum Tek. J. Tek. Mesin Terap.*, vol. 5, no. 1, pp. 26–30, 2023, doi: 10.18196/jqt.v5i1.19012.
- [7] I. Muhlisin and S. Sudiman, "Pengaruh Variasi Beban terhadap Faktor Kekuatan Rangka Sepeda dari Bahan AISI 1035 Steel (SS) dengan Simulasi Solidworks," *Briliant J. Ris. dan Konseptual*, vol. 9, no. 1, p. 236, 2024, doi: 10.28926/briliant.v9i1.1822.
- [8] M. Y. Wibowo, I. Maulana, A. A. Ghyferi, B. A. Kurniawan, and M. Nuril, "Perancangan Chassis Prototype Mobil Warak dan Simulasi Statik dengan Metode Finite Element Analysis," *J. Mek. Terap.*, vol. 3, no. 3, pp. 86–92, 2022, doi: 10.32722/jmt.v3i3.5138.
- [9] Sandy Suryady and Eko Aprianto Nugroho, "Simulasi Faktor Keamanan dan Pembebanan Statik Rangka Pada Turbin Angin Savonius," *J. Ilm. Multidisiplin*, vol. 1, no. 2, pp. 42–48, 2022, doi: 10.56127/jukim.v1i2.94.
- [10] F. A. Budiman, A. Septiyanto, Sudiyono, A. D. N. I. Musyono, and R. Setiadi, "Analisis Tegangan von Mises dan Safety Factor pada Chassis Kendaraan Listrik Febrian Arif Budiman dkk / Jurnal Rekayasa Mesin," *Rekayasa Mesin*, vol. 16, no. 1, pp. 100–108, 2021.
- [11] F. Schoenmakers *et al.*, "Tech United Eindhoven Team Description 2013 - Middle Size League," vol. 2011, 2013, [Online]. Available: <http://www.techunited.nl/media/files/TDP2013.pdf>
- [12] J. Arif, Pungkas Prayitno, and Halan Al Hafidh, "Analisis static pada aluminium 5052 dengan variasi sudut menggunakan solidworks," *TEKNOSAINS J. Sains, Teknol. dan Inform.*, vol. 10, no. 1, pp. 38–50, 2023, doi: 10.37373/tekno.v10i1.269.
- [13] Matweb, "MatWeb, Your Source for Materials Information," *MatWeb*, pp. 1–2, 2015, [Online]. Available: <http://www.matweb.com/search/datasheet.aspx?MatGUID=ff6d4e6d529e4b3d97c77d6538b29693>
- [14] M. I. Himawan, "Analisis Kekuatan Tarik Baja Karbon Rendah Dengan Metode Elemen Hingga Menggunakan Software (Solidwork)," *J. Ekon. Vol. 18, Nomor 1 Maret201*, vol. 2, no. 1, pp. 41–49, 2020.
- [15] P. Kurowski, "Engineering Analysis with SolidWorks Simulation 2019," *Eng. Anal. with SolidWorks Simul. 2019*, 2019, doi: 10.4271/9781630572372.
- [16] I. N. Agus Adi, K. R. Dantes, and I. N. P. Nugraha, "Analisis Tegangan Statik Pada Rancangan Frame Mobil Listrik Ganesha Sakti (Gaski) Menggunakan Software Solidworks 2014," *J. Pendidik. Tek. Mesin Undiksha*, vol. 6, no. 2, p. 113, 2018, doi: 10.23887/jjtm.v6i2.13046.

Performance Comparison of YOLOv5, YOLOv8, and YOLOv10 for Object Detection in Autonomous Soccer Robots

Rizqy Pratama Singarimbun^{1*}, Anugerah Wibisana¹, and ^{1*}

¹ Jurusan Teknik Elektro, Politeknik Negeri Batam, Indonesia

*Email: rizqy.pratama@students.polibatam.ac.id

Abstract—The Bareleng63 team designs autonomous soccer robots for the Wheeled Indonesian Soccer Robot Contest (KRSBI-Beroda), where efficient object detection is crucial. This study compares YOLOv5, YOLOv8, and YOLOv10 models, optimized using NVIDIA’s TensorRT, to assess their performance in terms of speed, accuracy, and robustness across varying conditions. YOLOv5 demonstrates over 90% accuracy within 1–3 meters, but its performance declines significantly beyond 6 meters, especially under low-light conditions. In contrast, YOLOv8 offers more stable performance, achieving above 70% accuracy up to 9 meters, making it more suitable for medium- to long-range detection. YOLOv10 outperforms both models, maintaining consistent accuracy up to 10 meters, even in challenging lighting conditions. In terms of inference speed, YOLOv5 exhibits the fastest average time (2.16 ms), followed by YOLOv8 (2.58 ms), and YOLOv10 (2.84 ms). YOLOv10 also excels in postprocessing time (0.097 ms), while YOLOv8 shows the slowest performance (0.316 ms). Regarding GPU resource utilization, YOLOv5 is the most efficient (22.5%), while YOLOv8 provides a balanced performance (24.5%), and YOLOv10 requires the most computational resources (25.8%). These findings highlight YOLOv10 as the most reliable choice for tasks demanding high accuracy and robustness, YOLOv5 as the optimal solution for systems with limited resources, and YOLOv8 as a well-rounded model that balances performance with efficiency.

I. INTRODUCTION

The Bareleng63 team is dedicated to creating autonomous wheeled soccer robots that take part each year in the Indonesian Robot Contest (Kontes Robot Indonesia, KRI), which is organized by PUSPRESNAS [1]. A category featured in this competition is the Wheeled Indonesian Soccer Robot Contest (KRSBI-Beroda), where teams are tasked with creating robots that can communicate, coordinate, and play soccer autonomously[2]. In this intricate setting, the ability to detect and track objects is essential for robots to accurately identify, find, and react to objects[3].

In the earlier system, object detection relied on color segmentation through OpenCV. While this method is quicker in computation, it has drawbacks, including sensitivity to lighting variations and challenges in differentiating objects with

comparable colors. To tackle these issues, a deep learning method utilizing the YOLO (You Only Look Once) algorithm was chosen. It provides enhanced accuracy and resilience, enabling it to identify and differentiate objects more consistently in diverse conditions[4].

To ensure real-time performance, TensorRT, NVIDIA’s inference library, was used to optimize deep learning models for edge devices. It streamlines models, reduces redundant parameters, and enhances efficiency with features like layer fusion, FP16 precision, and parallel execution. These optimizations accelerate inference while maintaining accuracy, making TensorRT vital for real-time applications.

This research evaluates YOLOv5, YOLOv8, and YOLOv10 by examining their inference speed, detection accuracy, and ability to handle varying lighting conditions. The TensorRT-optimized versions of these models are evaluated with the hope that this research will provide insights into which model offers the best balance of speed, accuracy, and robustness under various lighting conditions in robot soccer.

II. METHOD

A. YOLO Network Architecture

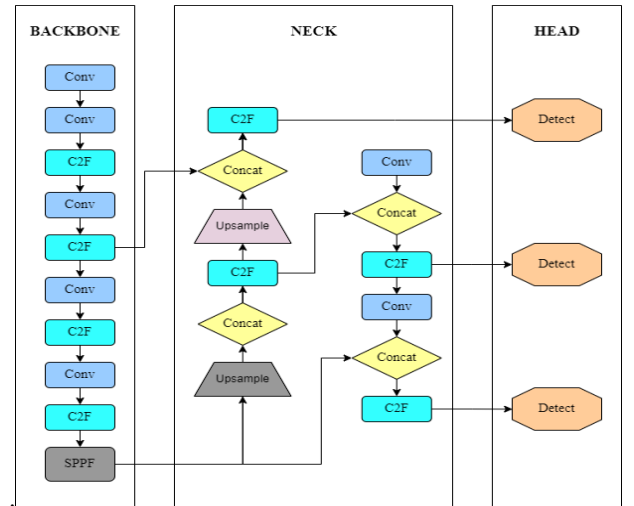


Fig. 1. YOLO Network Architecture

According to Figure 1, there are three principal components, specifically:

1) Backbone

The backbone is the first component of the YOLO network, tasked with capturing key features from the input image. Generally, the backbone is a deep convolutional neural network (CNN) that detects patterns, textures, and fundamental shapes in the image [5]. The main function of the backbone is to generate a feature map that holds encoded details about the objects and their positions within the image.

2) Neck

The neck serves as a connection between the head and the backbone of the YOLO network [6]. It improves the characteristics gathered by the backbone to render them more resilient for object detection.

3) Head

The head represents the last stage in the YOLO architecture, where detection takes place. It analyzes the feature map from the neck and estimates bounding boxes, class scores, and confidence scores for every object in the image [7].

B. TensorRT

TensorRT, developed by NVIDIA, is a high-performance inference engine designed to optimize and accelerate neural network models on NVIDIA GPUs. It achieves this through advanced optimizations such as layer fusion, kernel auto-tuning, and precision calibration (including FP16 and INT8), significantly reducing latency and boosting throughput.

To deploy a model with TensorRT, the process typically begins by exporting the trained model from the framework (like TensorFlow or PyTorch) to the ONNX format, an open standard that supports interoperability across frameworks. Once in ONNX format, TensorRT can import the model and generate an optimized engine for the target GPU. This engine is then ready for efficient inference on NVIDIA GPU platforms, such as NVIDIA GPUs or Jetson devices.

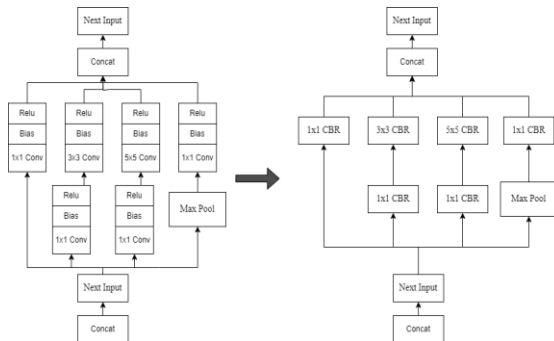


Fig. 2. Original network and network after get optimized in vertical

Figure 2 compares the original network and the optimized network vertically. On the left, the original network has a complex structure with multiple branches containing convolution operations (1x1, 3x3, 5x5) with ReLU activation and bias. In addition, there is a Max Pooling operation that

contributes to feature extraction. After optimization, as shown on the right, the network structure becomes more organized and simpler by replacing some convolution and activation blocks with CBR (Convolution-BatchNorm-ReLU) blocks. This reduces redundancy in data processing, improves computational efficiency, and maintains network performance.

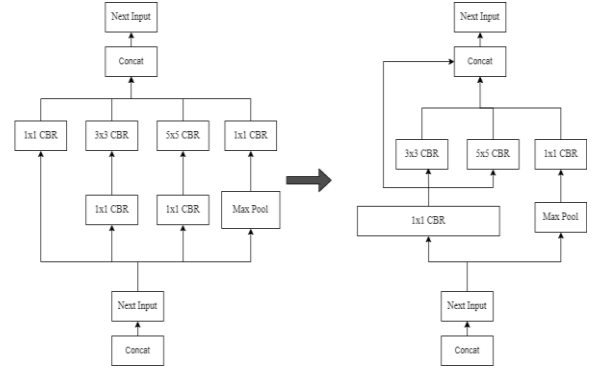


Fig. 3. Optimized vertical network and network after get optimized horizontal

Figure 3 shows a further optimization step by restructuring the network horizontally. Previously, the network elements were still arranged vertically, but after optimization, some blocks were combined and rearranged to reduce the depth of the network. This way, data propagation becomes more efficient, reduces computational complexity, and speeds up inference without losing important features.

C. Data Collection, Labeling, and Training Methodology

This section describes the approach used to collect, annotate, and train the model on the dataset utilized in this project. This procedure involves three key phases:

1) Data Collection

To guarantee strong model performance, datasets are gathered to reflect a range of real-world scenarios. Data was gathered using a ZED 2i camera that has a resolution of 672x376 pixels, and data was captured at different distances and positions, amounting to 3995 samples with two classes: balls and robots. This phase seeks to gather an extensive collection of images to encompass the diverse array of situations the model might face in real-world applications.

2) Labeling



Fig. 4. Result of Labeling in Roboflow

After gathering the dataset, Roboflow was used to annotate and prepare the images for training. This entails tagging every target item in the image to form a well-organized dataset appropriate for supervised learning as shown in Figure 4.

In addition to annotations, Roboflow's preprocessing features were applied to ensure that the dataset was consistent and met the model's input requirements. Images were resized to match the model's required input dimensions, ensuring uniformity across the dataset for optimal performance during training.

To further increase the dataset's robustness, specific data augmentation techniques including saturation and brightness adjustments were applied. By varying the visual properties of the images, different environmental conditions were effectively simulated, such as changes in lighting and color intensity. This augmentation strategy expands the dataset's diversity without additional data collection, producing images that represent a broader range of possible real-world scenarios [8].

These augmented variations help the model generalize more effectively by exposing it to a wider range of visual inputs. As a result, the model can perform reliably when encountering new, unseen data in deployment, ultimately improving both its accuracy and efficiency [9]. By enhancing the dataset in this way, we aimed to maximize model performance while minimizing the risk of overfitting to specific conditions present in the original dataset.

3) Training

```

yolo task=detect mode=train model=yolov8n.pt data=/content/data.yaml epochs=100 imgsz=672 batch=80 project=/content/drive/MyDr

```

Epoch	GPU_mem	box_loss	cls_loss	dfl_loss	Instances	Size
1/100	12.1G	1.319	2.764	0.9789	256	672: 100% 44/44 [01:09:00:00, 1.57s/it]
	Class	Images	Instances	Box(P	R	mAP50 mAP50-95): 100% 4/4 [00:10:00:00, 2.51s/it]
	all	497	1725	0.00517	0.564	0.6941 0.8346
Epoch 2/100	11.7G	1.12	1.155	0.929	279	672: 100% 44/44 [01:06:00:00, 1.51s/it]
	Class	Images	Instances	Box(P	R	mAP50 mAP50-95): 100% 4/4 [00:09:00:00, 2.49s/it]
	all	497	1725	0.00845	0.81	0.68 0.478
Epoch 3/100	11.8G	1.098	0.9038	0.9288	333	672: 100% 44/44 [01:03:00:00, 1.45s/it]
	Class	Images	Instances	Box(P	R	mAP50 mAP50-95): 100% 4/4 [00:07:00:00, 1.94s/it]
	all	497	1725	0.945	0.865	0.951 0.633
Epoch 4/100	11.8G	1.059	0.7485	0.923	219	672: 100% 44/44 [01:05:00:00, 1.48s/it]
	Class	Images	Instances	Box(P	R	mAP50 mAP50-95): 100% 4/4 [00:06:00:00, 1.51s/it]
	all	497	1725	0.953	0.927	0.957 0.627
Epoch 5/100	11.8G	1.046	0.6555	0.9197	310	672: 100% 44/44 [01:05:00:00, 1.50s/it]
	Class	Images	Instances	Box(P	R	mAP50 mAP50-95): 100% 4/4 [00:06:00:00, 1.64s/it]
	all	497	1725	0.963	0.906	0.955 0.66
Epoch 6/100	11.9G	1.013	0.5984	0.9124	258	672: 100% 44/44 [01:07:00:00, 1.54s/it]
	Class	Images	Instances	Box(P	R	mAP50 mAP50-95): 100% 4/4 [00:08:00:00, 2.13s/it]

Fig. 5. Log from the terminal showing model training progress in Google Colab.

Training the model took place on Google Colab with the free T4 GPU, striking a good balance between performance and efficiency for training with limited resources. Figure 5 shows the terminal logs during this training process, utilizing cloud infrastructure for processing. The T4 GPU can handle larger batch sizes, which results in faster training convergence. Nevertheless, if the VRAM is not enough for the batch size needed, upgrading to Colab Pro is suggested as it enables quicker training with support for bigger batch sizes[10].

The input image dimensions were configured to 672x672 pixels, providing a balanced compromise between computational demand and model precision. Bigger image sizes would capture more detailed features but demand considerably more memory and processing capability. Reduced image sizes, though more efficient, might compromise critical details [11]. The chosen image size offered ample detail without excessively straining the system's resources.

Training was conducted for 100 epochs, enabling the model to recognize patterns in the data and attain consistent performance. Typically, each training session lasted around 2 hours and 40 minutes.

4) Robot



Fig. 6. Omniwheel Robots

The omniwheeled soccer robot used in this study is equipped with omnidirectional and stereo cameras, essential for object detection, navigation, and decision-making. Omnidirectional cameras provide a 360-degree field of view, eliminating blind spots and helping the robot maintain situational awareness, track the ball, and identify other players. Meanwhile, stereo cameras, using two lenses spaced apart, generate depth perception by comparing images from each lens, allowing the robot to gauge distances and maneuver with precision accurately. For this study, only stereo cameras are used, as they provide the necessary depth information for precise navigation and object detection during gameplay. Figure 6 shows the overall design of the soccer robot used in this research..

III. RESULT

TABLE I
HARDWARE SPECIFICATION

Hardware	Description
GPU	Nvidia RTX 2060 Mobile 6GB
CPU	Intel Core i7 12 th Gen
RAM	16 GB

This study makes use of a device with an NVIDIA RTX 2060 Mobile 6GB GPU, an Intel Core i7 12th Gen processor, 16 GB of RAM, and runs on Ubuntu 22.04 as shown in Table 1. The version of TensorRT employed for optimizing the model is 8.6 and CUDA version 10.2 was used for accelerating the GPU.

A. Accuracy Test

TABLE 2
ACCURACY IN NORMAL

Distance	YoloV5	YoloV8	YoloV10
1 meter	96.13%	93.83%	91.22%
2 meter	93.71%	89.18%	91.46%
3 meter	91.70%	86.66%	87.37%
4 meter	88.39%	88.77%	86.33%
5 meter	88.77%	86.91%	83.97%
6 meter	86.48%	74.33%	80.71%
7 meter	80.32%	74.22%	66.55%
8 meter	59.22%	81.54%	76.84%
9 meter	Unstable-detect	79.18%	69.86%
10 meter	no detection	Unstable-detect	66.19%

Based on the table 2, at closer distances, YOLOv5 shows higher accuracy than YOLOv8 and YOLOv10, with the highest value at 1 meter (96.13%). However, as the distance increases, the accuracy of these three models decreases. YOLOv8 performed better at certain distances, such as 8 meters, where its accuracy reached 81.54% compared to YOLOv5 (59.22%) and YOLOv10 (76.84%). On the other hand, YOLOv10 showed relatively stable accuracy up to 6 meters but dropped more significantly at longer distances. At 9 meters, YOLOv5 experienced unstable detection, while YOLOv8 could still detect with 79.18% accuracy. At 10 meters, YOLOv5 cannot detect objects, while YOLOv8 experiences unstable detection, and YOLOv10 still provides an accuracy of 66.19%.

TABLE 3
ACCURACY IN LOW LIGHT

Distance	YoloV5	YoloV8	YoloV10
1 meter	95.69%	93.65%	91.11%
2 meter	93.32%	88.74%	91.06%
3 meter	90.83%	85.90%	87.26%
4 meter	87.98%	88.04%	85.98%
5 meter	88.49%	86.28%	83.57%
6 meter	85.81%	70.64%	79.81%
7 meter	79.57%	66.97%	69.03%
8 meter	Unstable-detect	74.13%	75.65%
9 meter	no detection	69.49%	69.64%
10 meter	no detection	Unstable-detect	59.98%

Refer to the table 3, under low lighting conditions, YOLOv5 shows the best accuracy at close range, with the highest value of 95.69% at a distance of 1 meter, followed by YOLOv8 at 93.65% and YOLOv10 at 91.11%. However, as the distance increases, the accuracy of these three models tends to decrease. YOLOv8 excels at certain distances, such as at 8 meters, with an accuracy of 74.13%, better than YOLOv5 which does not detect objects, and YOLOv10 which reaches 75.65%. YOLOv10 also showed stability in accuracy at certain distances compared to YOLOv8, especially after 6 meters. At a distance of 9 meters, YOLOv5 did not detect the object, while YOLOv8 and YOLOv10 recorded an accuracy of 69.49% and 69.64% respectively. At a distance of 10 meters, YOLOv5 was again unable to detect objects, YOLOv8 experienced unstable

detection, while YOLOv10 still recorded an accuracy of 59.98%.

TABLE 4
ACCURACY IN HIGH LIGHT

Distance	YoloV5	YoloV8	YoloV10
1 meter	96.38%	93.59%	92.32%
2 meter	93.31%	89.40%	90.90%
3 meter	89.71%	86.74%	87.03%
4 meter	86.36%	87.54%	85.62%
5 meter	86.99%	87.40%	84.75%
6 meter	86.61%	79.20%	84.81%
7 meter	82.42%	74.95%	67.17%
8 meter	69.59%	82.05%	78.28%
9 meter	Unstable-detect	79.28%	70.29%
10 meter	no detection	Unstable-detect	57.47%

based on data from the table 4, under bright lighting conditions, YOLOv5 had the highest accuracy at close range, with a maximum value of 96.38% at a distance of 1 meter. On the other hand, YOLOv8 recorded an accuracy of 93.59%, and YOLOv10 obtained 92.32%. As the distance increased, the accuracy performance of the three models generally decreased. At certain distances, YOLOv8 excelled, such as at 8 meters with an accuracy of 82.05%, which was higher than that of YOLOv5 (69.59%) and YOLOv10 (78.28%). The YOLOv10 model also showed stability in accuracy at several distances, especially up to 6 meters. At 9 meters, YOLOv5 could not detect consistently, while YOLOv8 and YOLOv10 recorded accuracies of 79.28% and 70.29%, respectively. At the farthest distance of 10 meters, YOLOv5 failed to detect the object, YOLOv8 experienced unstable detection, and YOLOv10 was still able to record an accuracy of 57.47%.



Fig. 7. (a) Low light, (b) High light, (c) Normal Light

This Figure. 7. (a) Low light, (b) High light, (c) Normal Light, shows the “ball” object recognition process under three different lighting conditions: low light, high light, and normal light. In the first frame, minimal lighting (low light) makes the object look less clear, which can decrease the detection accuracy. In the second frame, very bright lighting (high light) can cause object details to be overexposed, although confidence remains high. Meanwhile, the third frame features more balanced lighting (normal light), resulting in optimal detection as the object looks clearer. The variation in confidence at 79.22, 82.42, and 81.22 shows how changes in lighting affect the confidence level of the model in detecting objects. The same background in all three frames shows that the difference in results is entirely influenced by the lighting conditions, not by other environmental factors.

B. Speed test

TABLE 5
POSTPROCESS SPEED

Iteration	YoloV5	YoloV8	YoloV10
1	0.1693	0.3218	0.0986
2	0.1673	0.3172	0.0973
3	0.167	0.3153	0.0995
4	0.1737	0.3171	0.0965
5	0.1672	0.3096	0.0964
6	0.1674	0.3131	0.0976
7	0.1706	0.3201	0.0906
8	0.1686	0.3121	0.0963
9	0.1602	0.3112	0.0969
10	0.1571	0.323	0.0977
Average	0.16684ms	0.31605ms	0.09674ms

Table 5 shows the postprocess speed comparison between YoloV5, YoloV8, and YoloV10 in 10 iterations. From the recorded results, YoloV10 has the fastest postprocess speed with an average of 0.09674 ms, followed by YoloV5 with an average of 0.16684 ms, and YoloV8 with an average of 0.31605 ms. This shows that YoloV10 is more efficient in the postprocess stage compared to previous versions, with a significant time difference.

TABLE 6
INFERENCE SPEED

Iteration	YoloV5	YoloV8	YoloV10
1	2.1767	2.5559	2.835
2	2.1761	2.5631	2.8156
3	2.1745	2.5624	2.8233
4	2.1678	2.5874	2.8577
5	2.1697	2.5989	2.861
6	2.187	2.5826	2.8176
7	2.1833	2.57	2.8139
8	2.1654	2.5906	2.8522
9	2.1212	2.5956	2.867
10	2.1202	2.5889	2.8493
Average	2.16419ms	2.57954ms	2.83926ms

Table 6 compares the inference speed for the three versions of Yolo in 10 iterations. YoloV5 shows an average inference time of 2.16419 ms, while YoloV8 records an average time of 2.57954 ms, and YoloV10 has an average time of 2.83926 ms. From this data, it can be seen that YoloV5 has the fastest inference performance, followed by YoloV8, while YoloV10 takes the longest inference time. This indicates that although YoloV10 excels in postprocess speed, the time required for inference is greater compared to previous versions.

Combined, YoloV5 has the best performance with the fastest total average time of 2.33098 ms, combining postprocess and inference. YoloV8 is in the middle with a higher total time, but offers a balance between speed and accuracy. Meanwhile, YoloV10, despite excelling in postprocess, has the slowest total time of 2.936 ms, due to its longer inference time. This

comparison shows that model selection depends on the specific need between speed or accuracy.

C. GPU utilization

TABLE 7
GPU UTILIZATION

Iteration	YoloV5	YoloV8	YoloV10
1	25	26	28
2	24	26	26
3	22	25	26
4	22	24	25
5	22	24	25
6	22	24	25
7	22	24	26
8	22	24	25
9	22	24	26
10	22	24	26
Average	22.5%	24.5%	25.8%

Based on Table 7, YOLOv10 exhibits the highest average GPU utilization (25.8%), followed by YOLOv8 (24.5%) and YOLOv5 (22.5%). This indicates that YOLOv10 demands greater computational resources, likely due to improved accuracy or advanced features, though this comes with increased power consumption and thermal output. In contrast, YOLOv8 strikes a balance between performance and efficiency, while YOLOv5 has the lowest resource requirements, making it ideal for systems with limited computational capacity.

IV. CONCLUSION

In conclusion, YOLOv5 excels in fast inference times and low GPU utilization, making it an ideal choice for systems with limited computational resources. However, its performance tends to degrade beyond 7 meters, especially in low-light conditions, limiting its effectiveness for long-range detection or in darker environments.

On the other hand, YOLOv8 strikes a balance between accuracy and resource consumption, providing consistent results up to 8 meters. This comes at the cost of slower processing times compared to YOLOv5, making it a better option for applications that require stable performance within medium-range distances.

Lastly, YOLOv10 stands out as the most reliable solution for accurate detections across varying distances and lighting conditions. Despite its higher computational resource demands, YOLOv10 excels in tasks requiring high precision, both in low-light and well-lit environments, and at longer distances than the other versions.

Overall, the choice between YOLOv5, YOLOv8, and YOLOv10 depends on the specific needs of the application, with YOLOv5 excelling in speed, YOLOv8 offering a balanced trade-off between accuracy and efficiency, and YOLOv10 being the top choice for high-accuracy tasks in diverse conditions.

ACKNOWLEDGMENT


The authors gratefully acknowledge the financial support received from Barelang Robotics and Artificial Intelligence (BRAIL) and the Electrical Engineering Department of Batam State Polytechnic. They also extend their appreciation to the Search and Rescue Robotics Research Team at BRAIL for their significant contributions and expertise throughout the project. Special acknowledgment is directed to Mr. Anugerah Wibisana, the Head Advisor, for his exceptional guidance and mentorship. Finally, the authors convey their heartfelt gratitude to their families, particularly their parents, for their steadfast support and motivation, which have been vital in the pursuit of their academic goals.

REFERENCES

- [1] H. Soebhakti *et al.*, “BARELANG63 Team Description 2023.” [Online]. Available: <https://brail.polibatam.ac.id/Barelang63/index.html>
- [2] B. Pengembangan Talenta, I. Pusat, P. Nasional, K. Pendidikan, and D. Teknologi, “PEDOMAN KONTES ROBOT INDONESIA (KRI) PENDIDIKAN TINGGI TAHUN 2024.”
- [3] C. Zhang, Z. Yang, L. Liao, Y. You, Y. Sui, and T. Zhu, “RPEOD: A Real-Time Pose Estimation and Object Detection System for Aerial Robot Target Tracking,” *Machines*, vol. 10, no. 3, Mar. 2022, doi: 10.3390/machines10030181.
- [4] S. Khalid, H. M. Oqaibi, M. Aqib, and Y. Hafeez, “Small Pests Detection in Field Crops Using Deep Learning Object Detection,” *Sustainability (Switzerland)*, vol. 15, no. 8, Apr. 2023, doi: 10.3390/su15086815.
- [5] K. Liu, L. Peng, and S. Tang, “Underwater Object Detection Using TC-YOLO with Attention Mechanisms,” *Sensors*, vol. 23, no. 5, Mar. 2023, doi: 10.3390/s23052567.
- [6] J. Terven, D. M. Córdova-Esparza, and J. A. Romero-González, “A Comprehensive Review of YOLO Architectures in Computer Vision: From YOLOv1 to YOLOv8 and YOLO-NAS,” Dec. 01, 2023, *Multidisciplinary Digital Publishing Institute (MDPI)*. doi: 10.3390/make5040083.
- [7] M. Hussain, “YOLOv5, YOLOv8 and YOLOv10: The Go-To Detectors for Real-time Vision,” Jul. 2024, [Online]. Available: <http://arxiv.org/abs/2407.02988>
- [8] M. Akrouf *et al.*, “Diffusion-based Data Augmentation for Skin Disease Classification: Impact Across Original Medical Datasets to Fully Synthetic Images,” Jan. 2023, [Online]. Available: <http://arxiv.org/abs/2301.04802>
- [9] L. Li and M. Spratling, “Data Augmentation Alone Can Improve Adversarial Training,” Jan. 2023, [Online]. Available: <http://arxiv.org/abs/2301.09879>
- [10] U. Sirisha, S. P. Praveen, P. N. Srinivasu, P. Barsocchi, and A. K. Bhoi, “Statistical Analysis of Design Aspects of Various YOLO-Based Deep Learning Models for Object Detection,” Dec. 01, 2023, *Springer Science and Business Media B.V.* doi: 10.1007/s44196-023-00302-w.
- [11] D. Chansong and S. Supratid, “Impacts of Kernel Size on Different Resized Images in Object Recognition Based on Convolutional Neural Network,” in *Proceeding of the 2021 9th International Electrical Engineering Congress, iEECON 2021*, Institute of Electrical and Electronics Engineers Inc., Mar. 2021, pp. 448–451. doi: 10.1109/iEECON51072.2021.9440284.

**FORMULIR LOGBOOK BIMBINGAN DAN PENGAJUAN
SIDANG TUGAS AKHIR**

Nama : Muhammad Imron Shodiq
 NIM : 4222101009
 Pembimbing I : Anugerah Wibisana S.Tr.T, M.Tr.T
 Judul : Performance Comparison of Wheeled Soccer Robot Frames Using Finite Element Analysis (FEA)

No	Hari/Tgl	Rincian Kegiatan	TTD Pembimbing I
1	Senin, 26 Agustus 2024	Pengajuan topik penelitian jurnal Tugas Akhir	
2	Jum'at, 30 Agustus 2024	Pengajuan Judul Jurnal Tugas Akhir	
3	Kamis, 05 September 2024	Pemilihan metode penelitian Tugas Akhir	
4	Selasa, 10 September 2024	Pengumpulan data awal dan pemodelan desain robot	
5	Rabu, 18 September 2024	Analisis material dan properti mekanis untuk simulasi FEA	
6	Senin, 23 September 2024	Pelaksanaan simulasi FEA pertama	
7	Selasa, 1 Oktober 2024	Evaluasi hasil simulasi dan perbaikan desain	
8	Kamis, 10 Oktober 2024	Simulasi FEA kedua dengan desain yang diperbarui	
9	Senin, 21 Oktober 2024	Analisis hasil akhir simulasi dan perbandingan performa	
10	Rabu, 30 Oktober 2024	Penulisan bab pembahasan dan analisis hasil	
11	Selasa, 5 November 2024	Penulisan kesimpulan proyek	
12	Kamis, 14 November 2024	Penyusunan draft akhir jurnal	
13	Senin, 25 November 2024	Revisi akhir berdasarkan masukan pembimbing	
14	Jum'at, 3 Desember 2024	Pengajuan jurnal final	

Berdasarkan hasil bimbingan yang telah dilaksanakan selama 5 bulan dan telah disetujui oleh dosen pembimbing, maka dengan ini saya mengajukan diri sebagai peserta Sidang Tugas Akhir.

Batam, 06 Januari 2025
 Muhammad Imron Shodiq











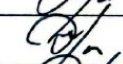


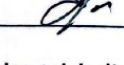
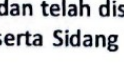

NIM : 4222101009

**Hapus yang tidak perlu.*

Jumlah bimbingan minimal 10 kali. Dalam satu minggu maksimal bimbingan yang dihitung adalah 2 kali.

**FORMULIR LOGBOOK BIMBINGAN DAN PENGAJUAN
SIDANG TUGAS AKHIR**

Nama : Rizqy Pratama Singarimbun
 NIM : 4222101004
 Pembimbing I : Anugerah Wibisana S.Tr.T, M.Tr.T
 Judul : Performance Comparison of YOLOv5, YOLOv8, and YOLOv10 for Object Detection in Autonomous Soccer Robots

No	Hari/Tgl	Rincian Kegiatan	TTD Pembimbing I
1	Senin, 26 Agustus 2024	Pengajuan topik penelitian untuk jurnal Tugas Akhir	
2	Jum'at, 30 Agustus 2024	Pengusulan judul jurnal Tugas Akhir	
3	Kamis, 05 September 2024	Pemilihan metode penelitian untuk Tugas Akhir	
4	Selasa, 10 September 2024	Revisi pada Bab 1 (Latar Belakang, Rumusan Masalah, serta Tujuan).	
5	Rabu, 18 September 2024	Revisi Bab 1 dengan menghubungkan penelitian sebelumnya dalam Latar Belakang.	
6	Senin, 23 September 2024	Revisi Bab 2 (Memperbaiki Jurnal Penelitian Terkait)	
7	Selasa, 1 Oktober 2024	Revisi Bab 2 (Menambahkan Narasi Untuk Menjelaskan Penelitian Yang Menjadi Rujukan)	
8	Kamis, 10 Oktober 2024	Revisi Proposal (tata letak gambar dan tabel)	
9	Senin, 21 Oktober 2024	Penyesuaian Judul Sesuai dengan masukan pembimbing	
10	Rabu, 30 Oktober 2024	Revisi Proposal (Koreksi Format Penulisan Huruf)	
11	Selasa, 5 November 2024	Penulisan kesimpulan proyek	
12	Kamis, 14 November 2024	Penyusunan draft akhir jurnal	
13	Senin, 25 November 2024	Revisi akhir berdasarkan masukan pembimbing	
14	Jum'at, 3 Desember 2024	Pengajuan jurnal final	

Berdasarkan hasil bimbingan yang telah dilaksanakan selama 5 bulan dan telah disetujui oleh dosen pembimbing, maka dengan ini saya mengajukan diri sebagai peserta Sidang Tugas Akhir.

Batam, 06 Januari 2025
 Rizqy Pratama Singarimbun



NIM : 4222101004

**Hapus yang tidak perlu.*

Jumlah bimbingan minimal 10 kali. Dalam satu minggu maksimal bimbingan yang dihitung adalah 2 kali.